

## **Surface Ligand-Directed Pair-wise Hydrogenation for Heterogeneous Phase Hyperpolarization**

*S. Glögger, A.M. Grunfeld, Y. N. Ertas, J. McCormick, S. Wagner and L.-S. Bouchard\**

# Supporting Information

## Contents

<b>S1</b> Materials and Methods	3
<b>S2</b> Synthetic procedures	3
<b>S3</b> Characterization of the nanoparticles	4
<b>S4</b> <i>Para</i> -hydrogen experiments	9
<b>S5</b> Particle recycling	10
<b>S6</b> References	12

# S1 Materials and Methods

## Chemicals

Hexachloroplatinic acid, sodium borohydride, absolute ethanol, cysteine and acetylcysteine were purchased from Sigma-Aldrich. D<sub>2</sub>O was purchased from Cambridge isotopes and all chemicals were used without further purification.

## Methods for the particle characterization

NMR spectra were recorded on a Bruker AV600 or on a Bruker 94/20 Biospec with 9.4 T. Transmission electron microscopy (TEM) was performed on a FEI Tecnai T12. Thermogravimetric analysis (TGA) was conducted using a Perkin Elmer Pyris Diamond TG/DTA from 25 °C to 650 °C. UV/vis characterization was performed on an Agilent 8453 UV-vis spectrophotometer.

## S2 Synthetic procedures

Unless otherwise noted, every synthetic step was performed under inert gas atmosphere.

### Synthesis of acetylcysteine-capped platinum nanoparticles (NAC@Pt)

98.4 mg (0.19 mmol) of hexachloroplatinic acid hexahydrate and 40.3 mg (0.25 mmol) of acetylcysteine were dissolved in 25 mL deoxygenated ultrapure water under argon atmosphere and stirred for 30 minutes. Subsequently, 74 mg (1.95 mmol) NaBH<sub>4</sub> dissolved in 3 mL ultrapure water was added over 1 minute under argon atmosphere. The brown suspension was stirred for an additional hour, for 3 hours under static vacuum and concentrated to near dryness. Particles were precipitated with 30 mL deoxygenated, absolute ethanol. After 30 minutes the ethanol was decanted and the particles dried under vacuum. Alternatively, the particles were centrifuged for 30 minutes and the supernatant decanted followed by drying under vacuum. Further purification can be achieved by resuspending the particles in water, centrifuging the suspension at 109 000 rpm for 5 hours in an ultracentrifuge and removing the supernatant solvent followed by drying in vacuum.

### Synthesis of cysteine-capped platinum nanoparticles (Cys@Pt)

98.4 mg (0.19 mmol) of hexachloroplatinic acid hexahydrate and either 23.0 mg (0.19 mmol) or 25.3 mg (0.21 mmol) of L-cysteine were suspended in 25 mL deoxygenated ultrapure water under argon atmosphere and stirred for 30 minutes. Subsequently, 74 mg (1.95 mmol) NaBH<sub>4</sub> dissolved in 3 mL ultrapure water was added over 1 minute under argon atmosphere. The brown suspension was stirred for an additional hour, for 3 hours under static vacuum and concentrated to near dryness. Particles were precipitated with 30 mL deoxygenated, absolute ethanol. After 30 minutes the ethanol was decanted and the particles dried under vacuum. Alternatively, the particles were centrifuged for 30 minutes and the supernatant decanted followed by drying under vacuum. If a platinum precursor to cysteine ratio of 1:1 was used, Cys1@Pt platinum particles were yielded and if a ratio of 1:1.1 was used, Cys1.1@Pt particles were obtained.

## S3 Characterization of the nanoparticles

### Particle distribution and UV/vis

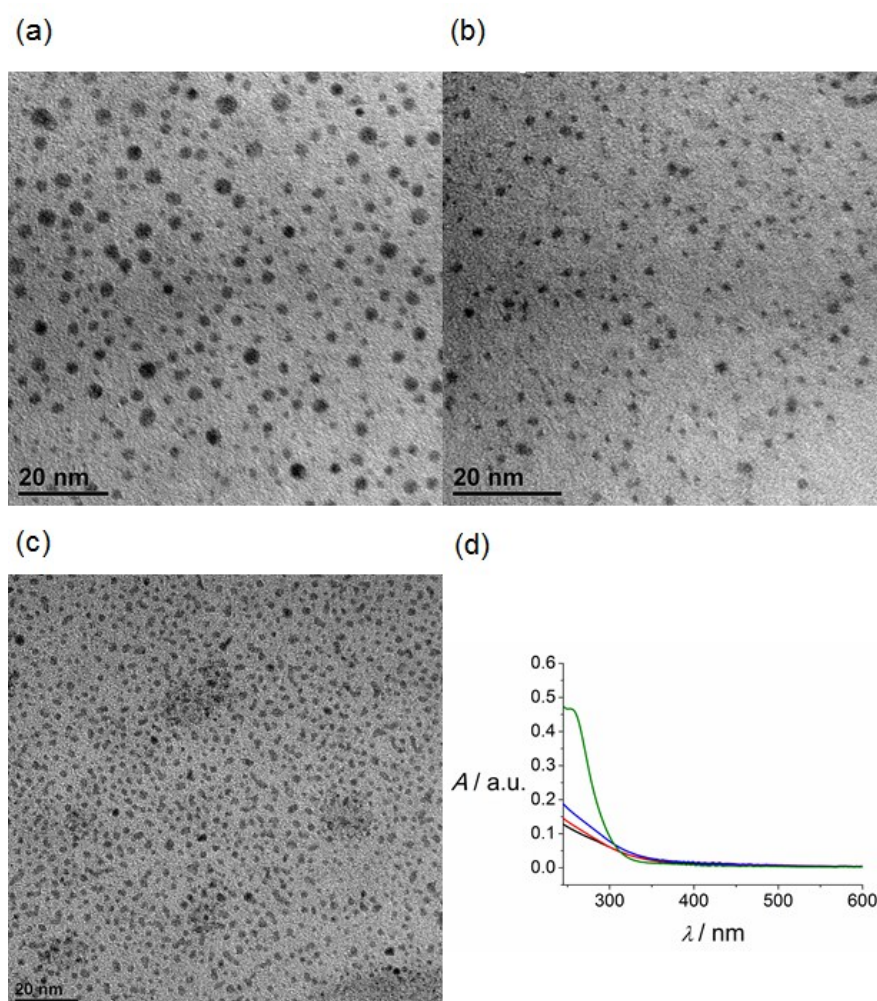


**Figure S1.** (a) TEM of the Cys1@Pt particles. (b) TEM of the Cys1.1@Pt particles. (c) TEM of the NAC@Pt particles. (d) UV/vis absorbance in water of hexachloroplatinic acid (green), Cys1.1@Pt (blue), NAC@Pt (red) and Cys1@Pt (black). The absence of the absorbance peak at 260 nm for the nanoparticle suspension shows that no platinum ions are present to catalyze a reaction.

Particle size distributions were determined for the three different particles. For NAC@Pt, Cys1@Pt and Cys1.1@Pt, 169, 187 and 134 particles were chosen at random. Sizes for the different particles of  $1.9 \pm 0.4$  nm,  $2.4 \pm 0.5$  nm and  $1.4 \pm 0.3$  nm were found. The given deviation corresponds to the standard deviation derived from a Gaussian fit over the particle size distribution. Histograms of the size distribution are shown in figure S2-S4.

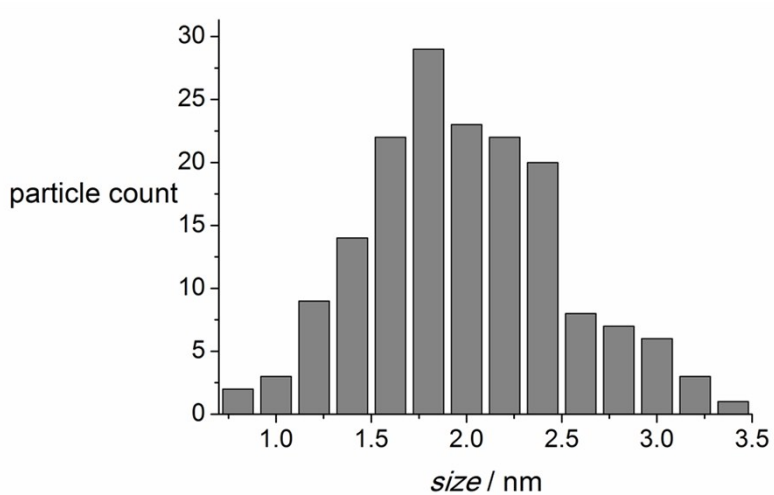


**Figure S2.** Nanoparticle distribution of NAC@Pt.

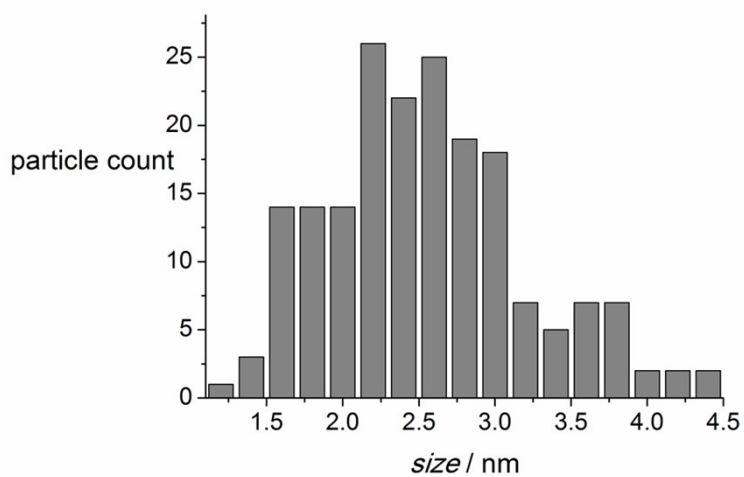


**Figure S3.** Nanoparticle distribution of Cys1@Pt.

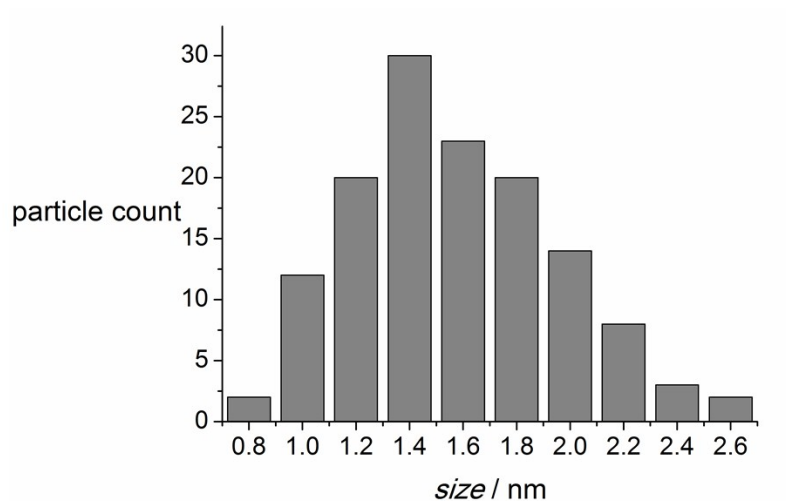


**Figure S4.** Nanoparticle distribution of Cys1.1@Pt.

### Thermogravimetric Analysis (TGA)

Thermogravimetric analysis was performed from 25°C to 650°C under argon. The TGA curves for the three particles are depicted in figure S5-7 and show that the surfaces of all the particles are 16 wt% covered.

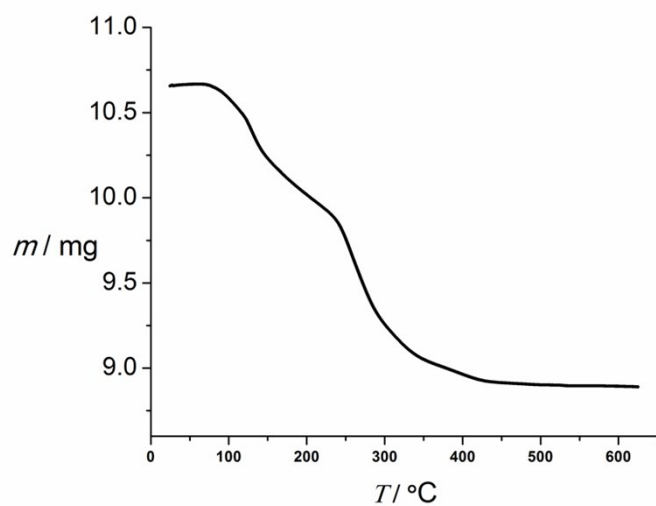


**Figure S5.** Thermogravimetric analysis of NAC@Pt.

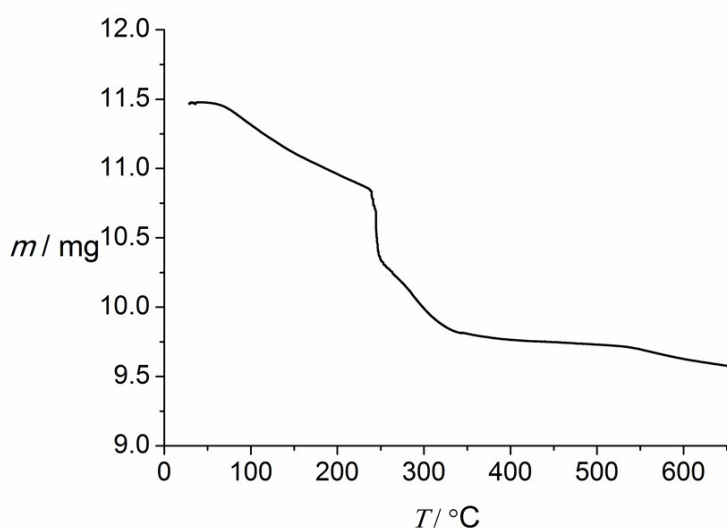


**Figure S6.** Thermogravimetric analysis of Cys1@Pt.

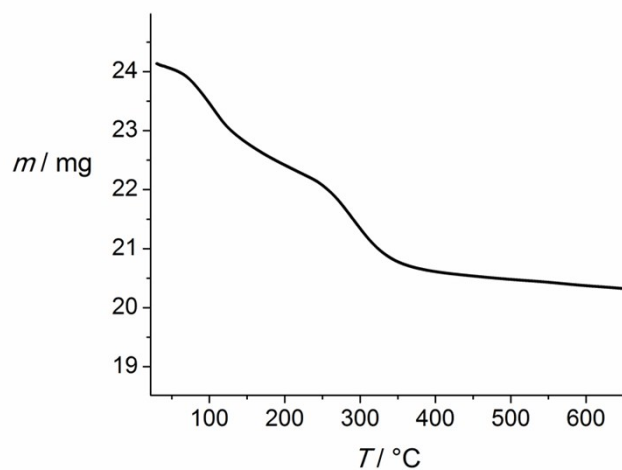


**Figure S7.** Thermogravimetric analysis of Cys1.1@Pt.

### **NMR of the particles**

In order to demonstrate that binding of the ligands to the particles has occurred,  $^1\text{H}$  NMR spectra were recorded at  $B_0=14.1$  T. A significant dipolar broadening of the peaks was observed due to the coordination to the nanoparticles for all three samples (Figures S 8-9).

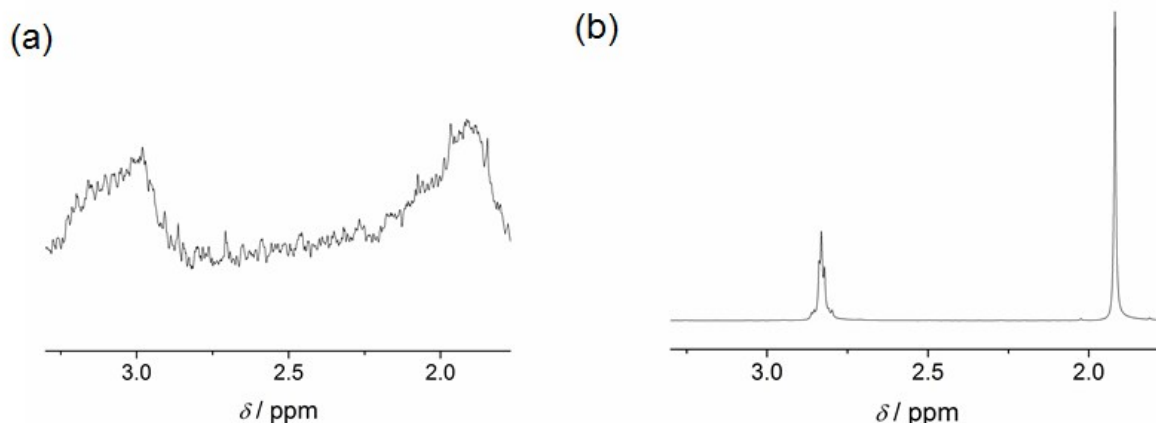


**Figure S8.**  $^1\text{H}$  NMR spectra of (a) NAC@Pt and (b) N-Acetylcysteine both in  $\text{D}_2\text{O}$ . The line broadening in (a) shows that the ligand is coordinated to the particles' surface.

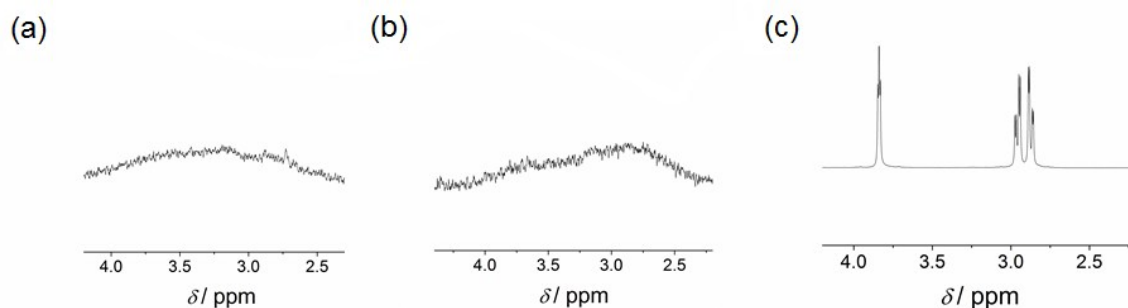


**Figure S9.**  $^1\text{H}$  NMR spectra of (a) Cys1@Pt, (b) Cys1.1@Pt and (c) cysteine in  $\text{D}_2\text{O}$ . The line broadening in (a) and (b) shows that the ligand is coordinated to the particles' surface.

### Mercury Poisoning

A mercury poisoning test was performed for all of the nanoparticles.<sup>[S1]</sup> In this experiment, added mercury forms amalgams with the platinum nanoparticles which results in catalytic deactivation. If the reaction is catalyzed by platinum ions rather than the particles, the reaction would progress since no deactivated amalgam is formed. For the test 2.0 mg of particles were suspended in 4 mL of water that contained an internal potassium acetate standard and 0.4 mL hydroxyethyl acrylate was added. Half of the solution was used for the poisoning test and half of it was used to run a control experiment without mercury. In both solutions, hydrogen was bubbled over 60 minutes with a flowrate of 100 mL/minute. Into one reaction 20  $\mu\text{L}$  of mercury were added after 15 minutes resulting in termination of the hydrogenation, whereas hydrogenation in the control experiment progresses (See figure S10-12). Thus the hydrogenation is catalyzed by the nanoparticles and not residual platinum ions.



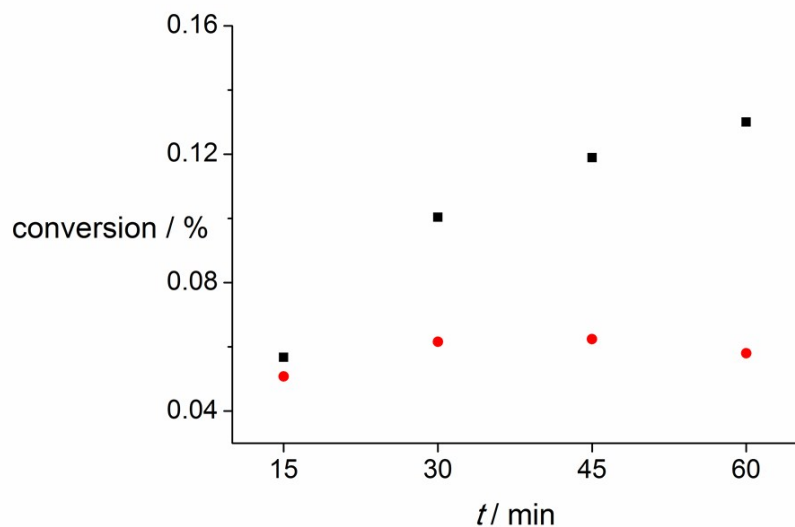


**Figure S10.** Mercury poisoning test of NAC@Pt. Without mercury the reaction progresses (black squares) whereas the reaction stops upon addition of mercury (red circles).

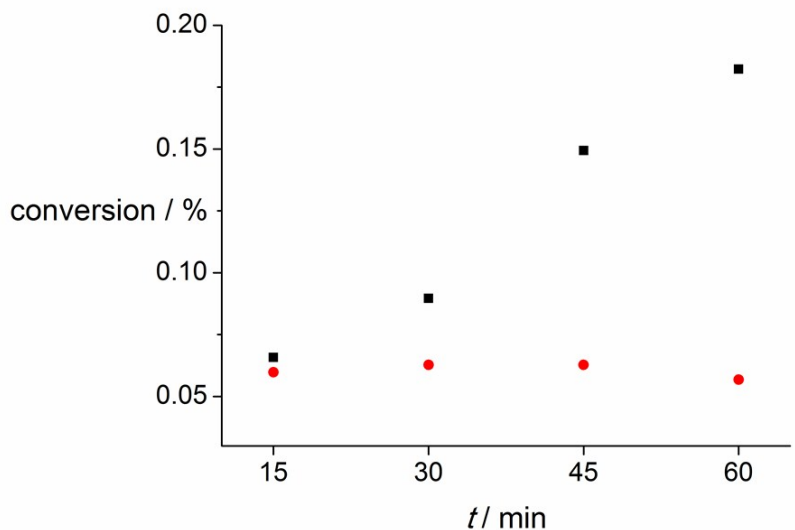


**Figure S11.** Mercury poisoning test of Cys1@Pt. Without mercury the reaction progresses (black squares) whereas the reaction stops upon addition of mercury (red circles).

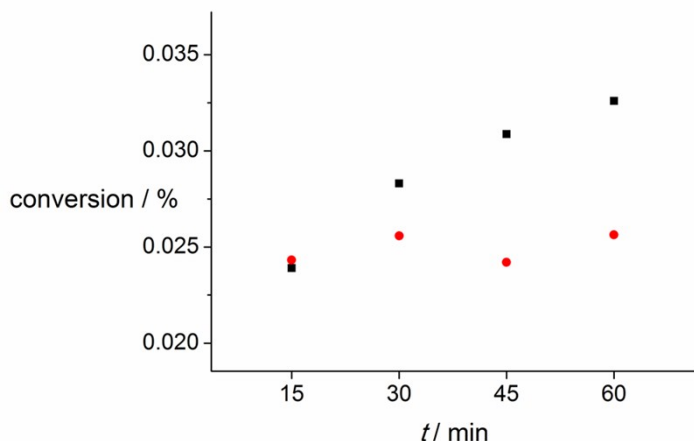


**Figure S12.** Mercury poisoning test of Cys1.1@Pt. Without mercury the reaction progresses (black squares) whereas the reaction stops upon addition of mercury (red circles).

### BET Measurements

BET Measurements on Cys1@Pt and NAC@Pt were performed by Quantachrome Instruments at 25°C with hydrogen gas. The results are summarized in table S1.

**Table S1.** Summary of BET measurement results

Particle	Active surface area / m <sup>2</sup> /g	Metal dispersion / %	Avg. crystallite size / nm
Cys1@Pt	0.417	16.9	6.7
NAC@Pt	0.202	8.2	13.8

The results suggest a much higher diameter of the particles than suggested by the TEM data. We attribute this difference to the way the samples are prepared and measured. For TEM measurements the particles are dispersed in water, and droplet is added on a TEM plate and the solvent is slowly evaporated. This leads to better dispersed particles as we expect it in solution during the PHIP experiments. For the BET measurements the particles are used in bulk powder form and thus less dispersed reflecting less precisely the catalytic system utilized. However one may conclude from the two different particle systems that the Cys1@Pt particles tend to be more dispersed with smaller crystallite size, which may lead to higher polarization, as the diffusion length of hydrogen on the platinum surface is smaller. The active metal dispersion and surface area are higher for the Cys1@Pt than for the NAC@Pt particles, which can be correlated with the turnover frequency (see table 1 in main article).

### S4 *Para*-hydrogen experiments

<sup>1</sup>H NMR experiments with para-hydrogen (95% para-enriched) were performed on a Bruker AV600 spectrometer ( $B_0 = 14.1$  T). Samples were prepared in 5 mm Young tubes from New Era that have been tested for blind activity before usage. Under inert gas 2 mg

hydroxyethyl acrylate (0.04 mmol) and various nanoparticle concentrations were suspended in 0.5 mL D<sub>2</sub>O. Each sample was heated to 80°C, pressurized with 5 bar of para-hydrogen, shaken in the earth's magnetic field (ALTADENA experiment) and transported into the center of the magnet within 5 s.<sup>[S2]</sup> The spectrum was recorded in a single scan (45°-pulse). After the hyperpolarization experiment, a spectrum was recorded with the formed product in thermal equilibrium, the signal enhancement and the corresponding polarization calculated. Various nanoparticle concentrations were used to determine the optimal particle concentration to generate the highest possible polarization and it was found to be 10 mg/mL for all of the tested particles (Figure S13). Each experiment was repeated at least 3 times. <sup>13</sup>C polarization experiments were performed on a custom-built polarizer at Cedars-Sinai Medical Center according to published procedures at 60°C.<sup>[S3]</sup> As before, the <sup>13</sup>C polarization achieved with the described polarizer was only a factor of 10 higher than in thermal equilibrium. Figure S14 compares the hyperpolarized signal with a signal in thermal equilibrium after 256 scans, showing that with the current polarizer setup no significant <sup>13</sup>C polarization could be achieved. Therefore, the construction of an optimized polarizer in conjunction with a heterogeneous catalyst, as described recently, is desirable.<sup>[S4]</sup>

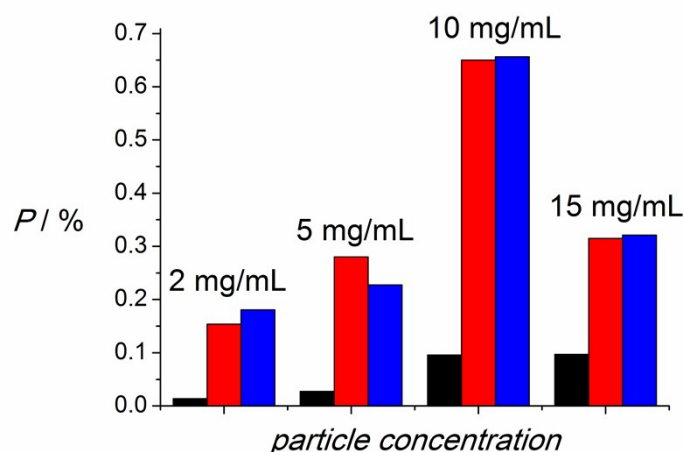


**Figure S13.** Polarization as a function of particle concentration: NAC@Pt (black), Cys1@Pt (red) and Cys1.1@Pt (blue).

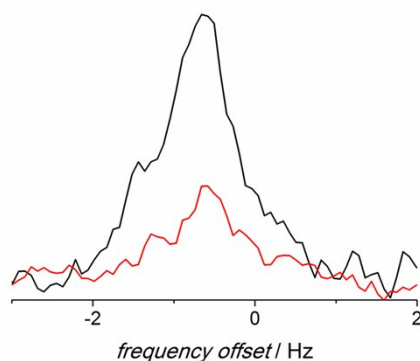


**Figure S14.** Thermal polarized signal of <sup>13</sup>C enriched HEP after 256 scans (black) and hyperpolarized signal (red, ten times magnified).

## S5 Particle Recycling

A further proof that the hydrogenation and thus hyperpolarization is catalyzed due to the nanoparticles is a recycling experiment. In this experiment 15 mg of particles were used to hyperpolarize HEP at 80°C and the hyperpolarized signal detected. Afterwards the particles were separated from the supernatant including the hydrogenated product in two different ways: Either by centrifuging the particles in D<sub>2</sub>O with 109 000 rotations per minute (rpm) for 2 hours in an ultracentrifuge, or by removing the solvent in vacuum followed by washing the particles with ethanol and drying them under vacuum again. Each of these experiments was performed twice for each particle. Afterwards the particles were reused up to four times following the same procedure. Over the course of the five performed experiments no significant loss in polarization was observed (Figure S15). To ensure that no significant amount of platinum has leached into the supernatant or that platinum ions dissolved in the solvent were in charge of the hyperpolarized signal, hyperpolarization experiments with the supernatant solvent were performed. To the supernatant from the polarization experiments, 2 mg HEA were added and a hyperpolarization experiment performed as above was conducted. Figure S16-18 show that for no particle a hyperpolarized signal could be observed. Therefore, it can be concluded that the polarization was indeed generated due to the platinum nanoparticle catalyst and that no significant leaching has occurred.

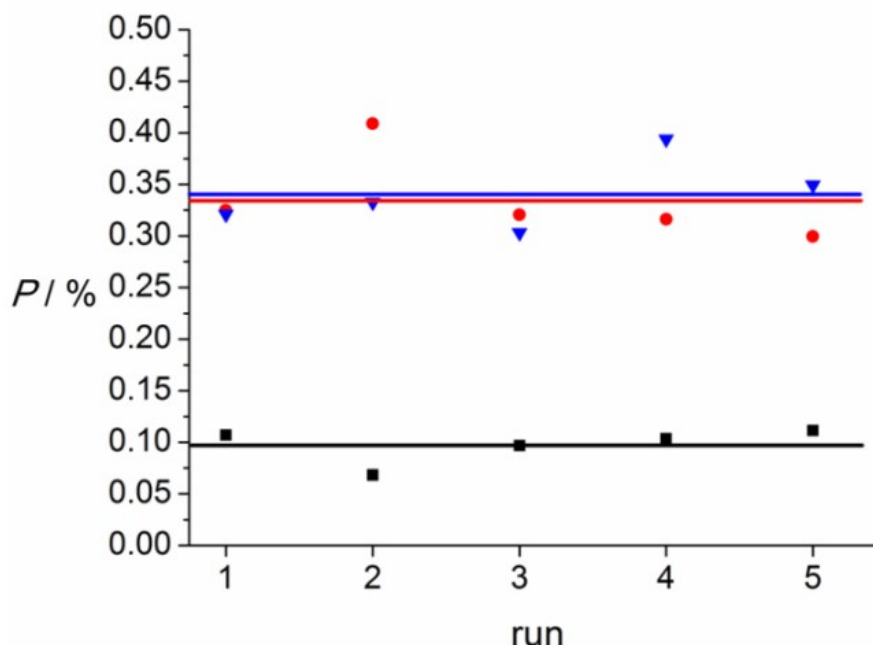


**Figure S15.** Particle recycling experiments with Cys1.1.Pt (blue triangles), Cys1@Pt (red circles) and NAC@Pt (black squares). The added lines represent the average polarization values achieved with each particle.

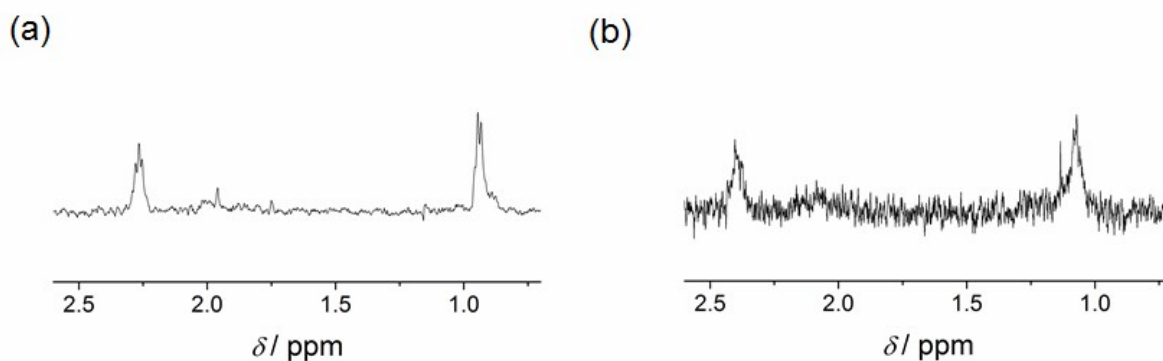


**Figure S16.** a)  $^1\text{H}$  spectrum of the product in the supernatant after separating NAC@Pt and the product in solution at  $B_0=14.1$  T. b)  $^1\text{H}$  spectrum of the hyperpolarization experiment after new HEA was added. The spectrum shows that no hyperpolarization pattern is observable and the thermal magnetization as not fully built up yet. Thus significant leaching of the catalyst is not observable.

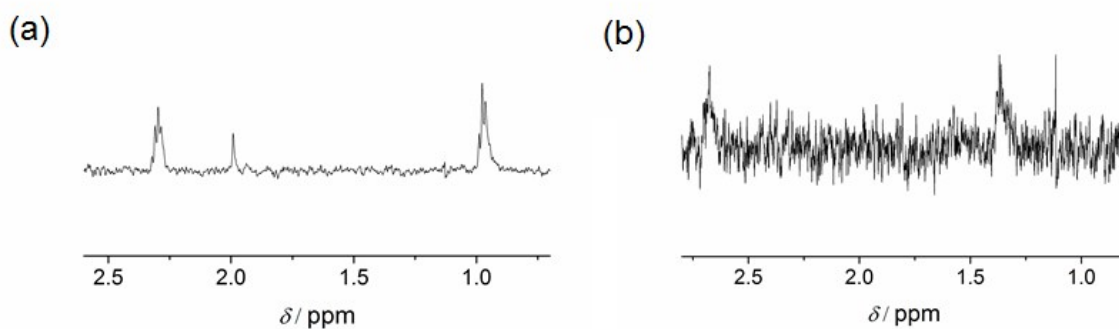


**Figure S17.** a)  $^1\text{H}$  spectrum of the product in the supernatant after separating Cys1@Pt and the product in solution at  $B_0=14.1$  T. b)  $^1\text{H}$  spectrum of the hyperpolarization experiment after new HEA was added. The spectrum shows that no hyperpolarization pattern is observable and the thermal magnetization as not fully built up yet. Thus significant leaching of the catalyst is not observable.

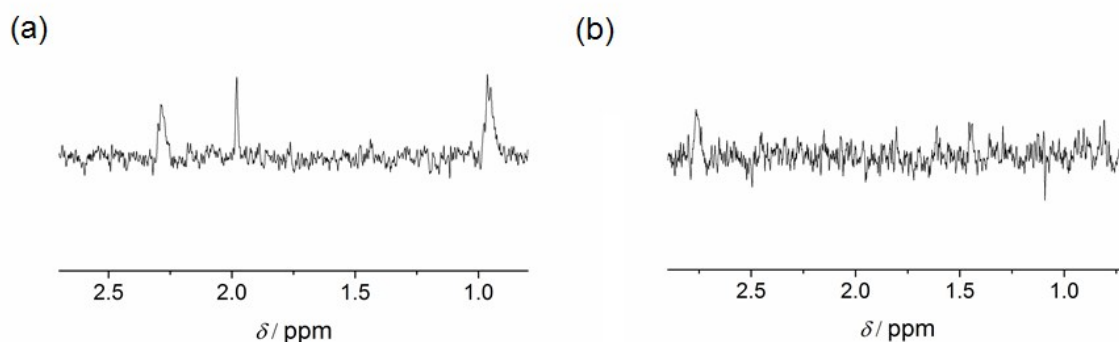


**Figure S18.** a)  $^1\text{H}$  spectrum of the product in the supernatant after separating Cys1.1@Pt and the product in solution at  $B_0=14.1$  T. b)  $^1\text{H}$  spectrum of the hyperpolarization experiment after new HEA was added. The spectrum shows that no hyperpolarization pattern is observable and the thermal magnetization as not fully built up yet. Thus significant leaching of the catalyst is not observable.

## S6 References

- S1 R. H. Crabtree, *Chem. Rev.*, 2012, **112**, 1536.
- S2 M. G. Pravica and D. P. Weitekamp, *Chem. Phys. Lett.*, 1988, **145**, 255.
- S3 J. Agraz, A. Grunfeld, K. Cunningham, D. Li and S. Wagner, *J. Magn. Reson.*, 2013, **235**, 77.
- S4 S. Glögler, A. M. Grunfeld, Y. N. Ertas, J. McCormick, S. Wagner, P. P. M. Schleker, L.-S. Bouchard, *Angew. Chem. Intl. Ed.*, 2015, **54**, 2452.